# Tunable magnetic exchange between rare-earth metal 5*d* and iron 3*d* states. A case study of the multiple magnetic transitions in $Gd_6FeBi_2$ and the solid solutions $Dy_{6-x}Gd_xFeBi_2$ ($1 \leq x \leq 5$) with Curie temperatures in the range 120–350 K

Jiliang Zhang,[a,b] Jey-Jau Lee,[c] Tonghan Yang,[d] Wei He,[d] Yong-Mook Kang,[b *] Svilen Bobev[a *]

[a] Department of Chemistry and Biochemistry, University of Delaware, Newark, DE 19716, United States of America

[b] Department of Materials Science and Engineering, Korea University, Seoul 02841, Republic of Korea

[c] National Synchrotron Radiation Research Center, Hsinchu 30076 Taiwan, Republic of China

[d] School of Resources, Environment and Materials, Guangxi University, Nanning 530004, Guangxi, Peoples Republic of China

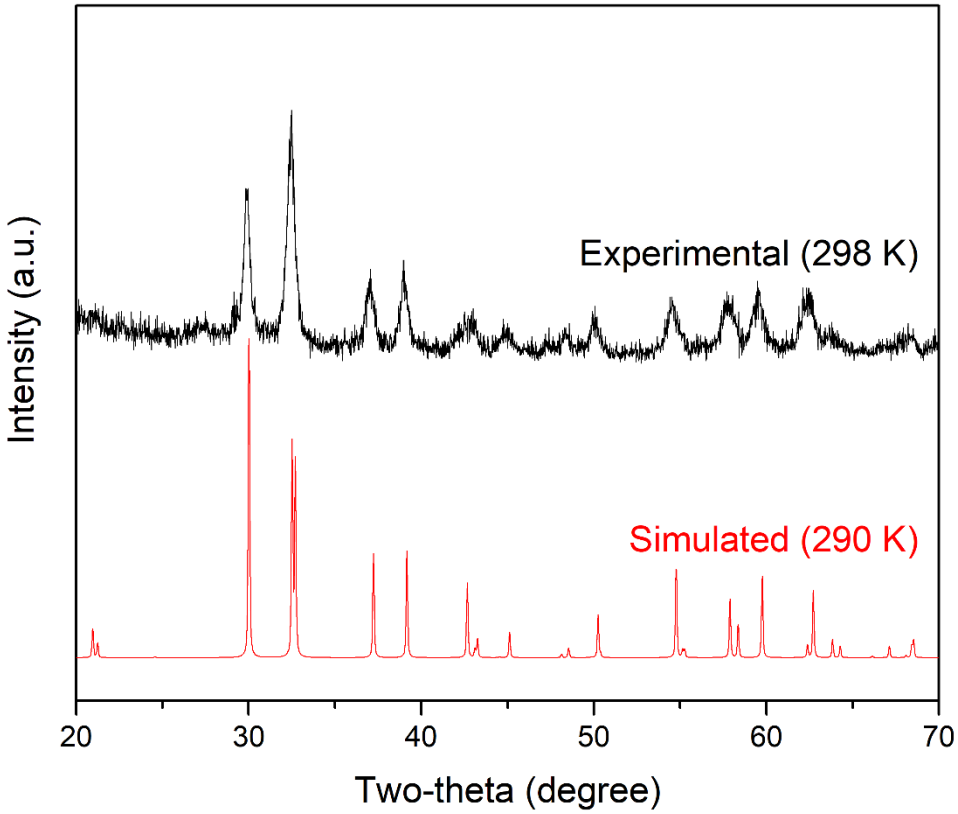


**Figure S1.** Experimental and simulated PXRD patterns of $Gd_6FeBi_2$. The slight peak shifts of experimental pattern towards low angle are due to the high temperature compared with the simulated pattern.

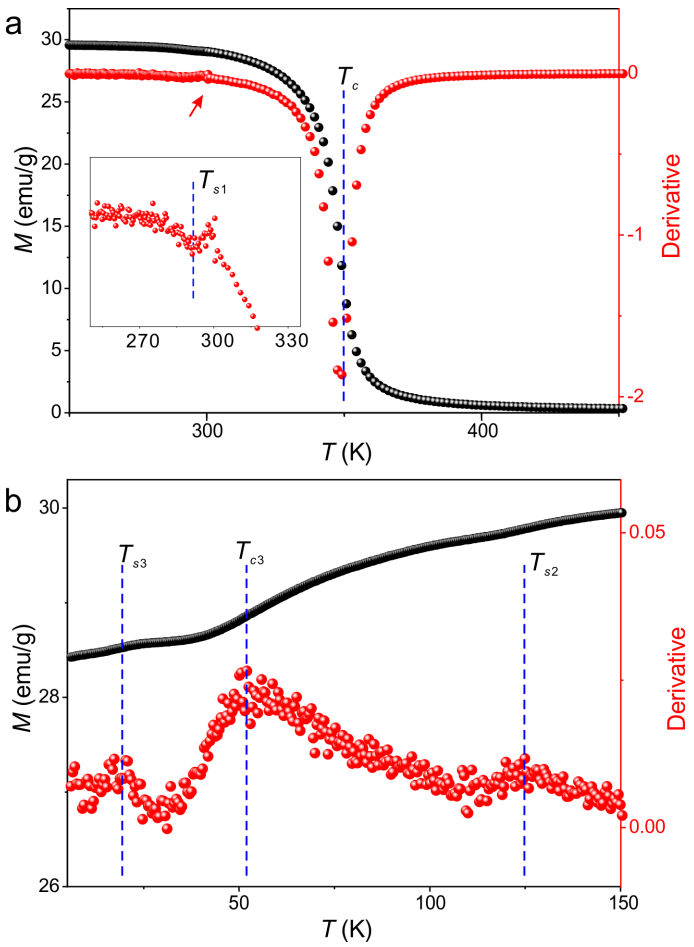


**Figure S2.** Temperature dependent magnetization $M$ (a) and its derivative (b) for $Gd_6FeBi_2$. In (a), the arrows mark the transitions and the insets show the determination of $T_{c2}$ and $T_{c3}$. The blue dash lines in (b) label the transitions determined by peak values of the derivative.

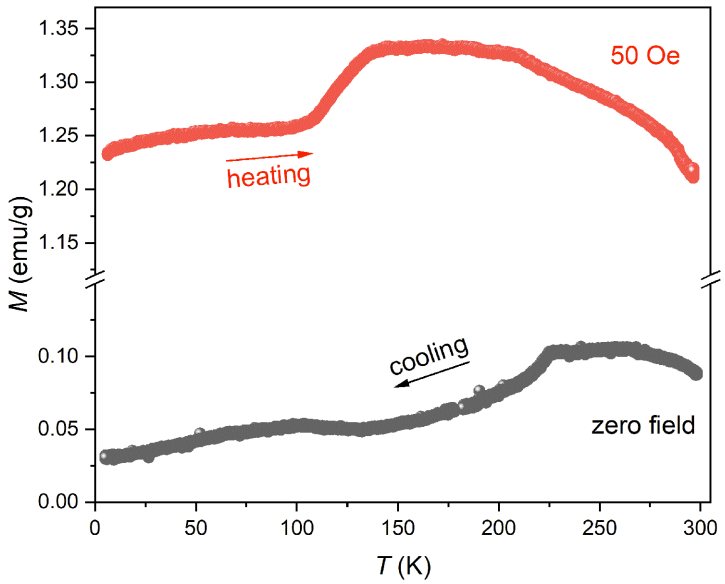


**Figure S3.** Temperature dependent magnetization (*M*) of $Gd_6FeBi_2$ in zero applied field (black), and under an applied field of 50 Oe (red).

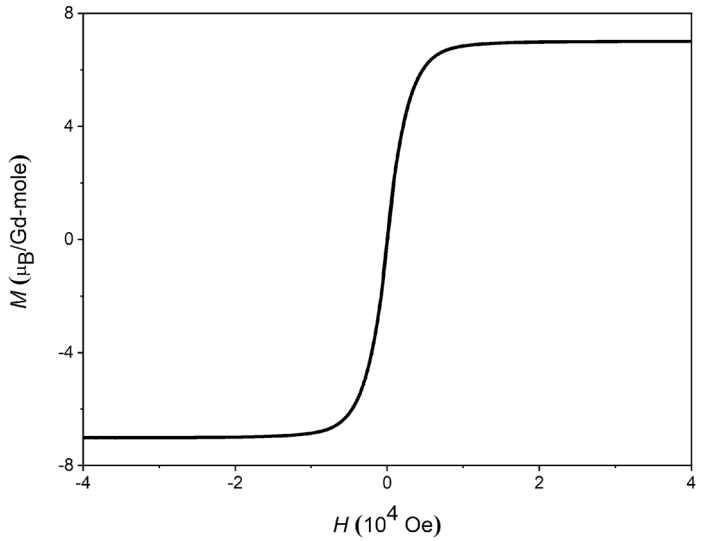


**Figure S4.** Field dependent magnetization (*M*) of $Gd_6FeBi_2$ at 5 K.

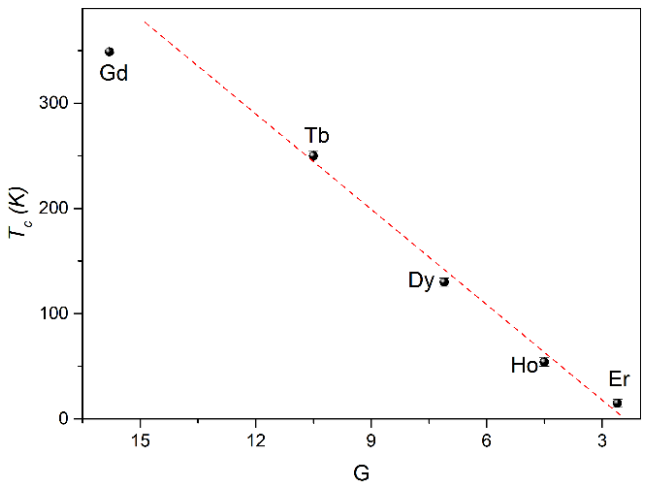


**Figure S5.** Curie temperatures of the $RE_6FeBi_2$ compounds, plotted as a function of the corresponding de Gennes factors.

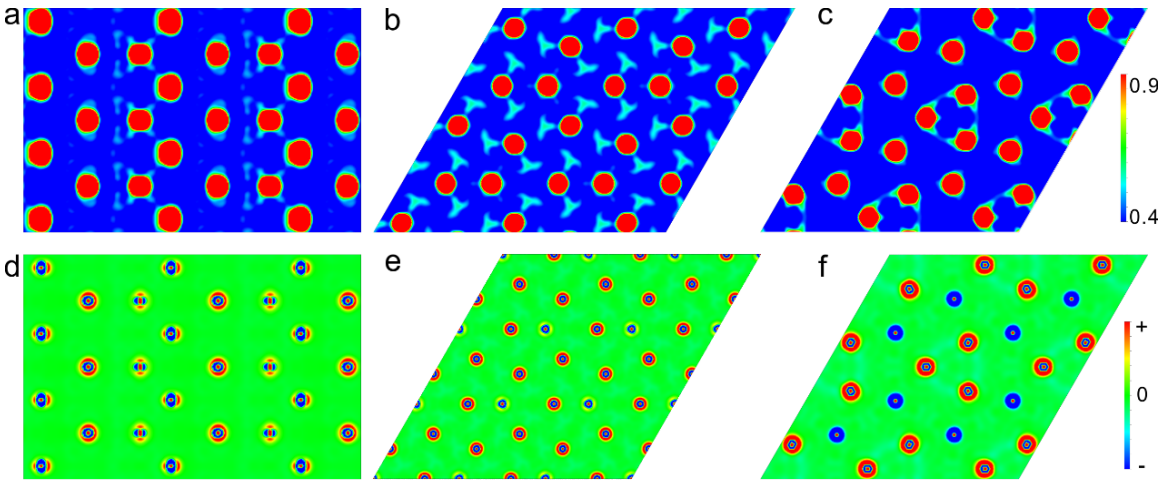


**Figure S6.** MEM electron density (a-c) and difference electron density maps (d-f) projected on lattice planes shown in Figure 5 (a, d for $x$=0; b, e for $z$=0; c,f for $z$=0.5). The unit in the legend for electron density is $e/a_0^3$ where $a_0$ is Bohr radius.

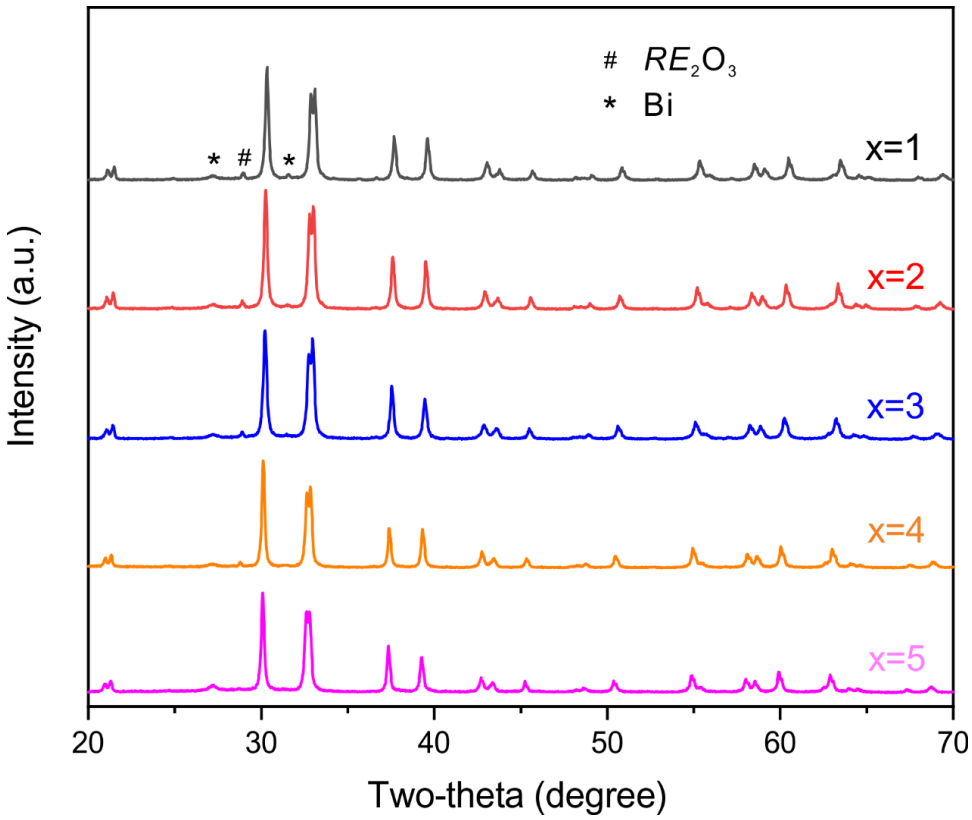


**Figure S7.** PXRD patterns of solid solutions $Dy_{6-x}Gd_xFeBi_2$ ($1 \leq x \leq 5$). The prepared samples apprear highly-crystalline and hoimogenous, with only tiny impurities of $RE_2O_3$ and Bi observed (labelled), and other peaks belong to the $Zr_6AlCo_2$-type structure**.**

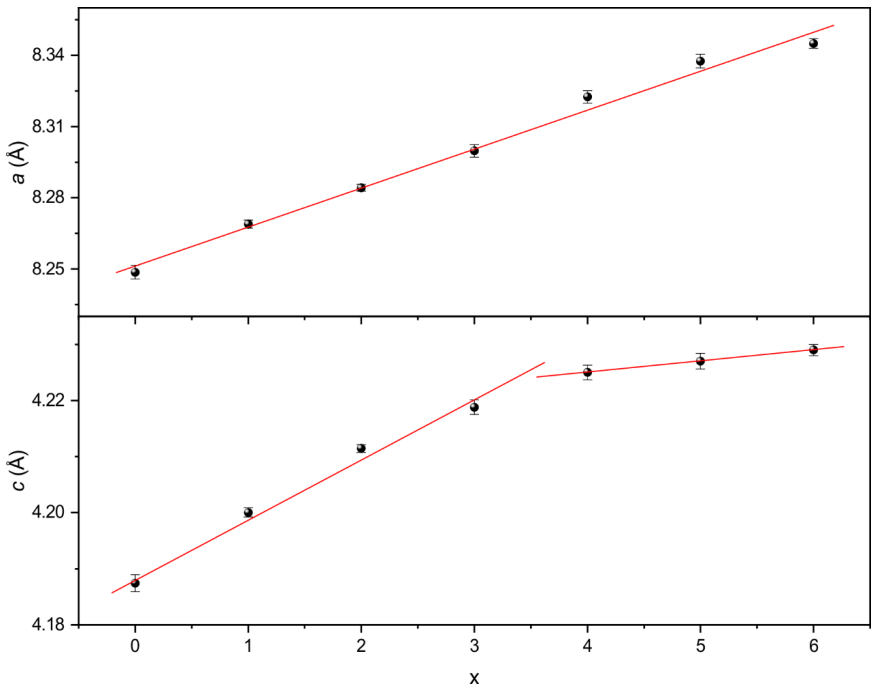


**Figure S8.** Variation of lattice parameters against Gd concentration in $Dy_{6-x}Gd_xFeBi_2$ ($1 \leq x \leq 5$) compounds. The solid lines show the linear data fitting of lattice parameters against Gd concentration.

**Table S1.** Selected Crystallographic Data for $Gd_6FeBi_2$ at different temperatures.

| Temperature (K) | 135 | 150 | 170 | 190 | 230 | 250 | 270 |
|---|---|---|---|---|---|---|---|
| Radiation | Mo Kα, λ = 0.71073 Å | | | | | | |
| Space group | $P\bar{6}2m$ (No. 189), $Z = 1$ | | | | | | |
| $a$ (Å) | 8.3343(16) | 8.337(4) | 8.3474(17) | 8.349(2) | 8.3512(14) | 8.3561(16) | 8.359(5) |
| $c$ (Å) | 4.2279(16) | 4.229(2) | 4.2339(9) | 4.2342(12) | 4.2343(8) | 4.2354(9) | 4.231(3) |
| $V$ (Å$^3$) | 254.33(12) | 254.5(2) | 255.48(9) | 255.58(12) | 255.75(8) | 256.11(11) | 256.0(3) |
| $\rho_{cal}$ (g cm$^{-3}$) | 9.254 | 9.246 | 9.210 | 9.208 | 9.202 | 9.189 | 9.192 |
| $\mu$ (cm$^{-1}$) | 742.70 | 742.10 | 739.15 | 739.06 | 738.58 | 737.53 | 737.76 |
| Final $R_1$ [$I > 2\sigma(I)$] | 0.0260 | 0.0234 | 0.0249 | 0.0215 | 0.0203 | 0.0218 | 0.0249 |
| Final $wR_2$ [$I > 2\sigma(I)$] | 0.0430 | 0.0392 | 0.0406 | 0.0372 | 0.0343 | 0.0433 | 0.0429 |

$R_1=\sum||F_o|-|F_c||/\sum|F_o|$; $wR_2=[\sum[w(F_o^2-F_c^2)^2]/\sum[w(F_o^2)^2]]^{1/2}$, where $w=1/[\sigma^2F_o^2+(AP)^2+(BP)]$, and $P=(F_o^2+2F_c^2)/3$; $A$, $B$ are the respective weight coefficients (see CIF).

**Table S2.** Atomic Coordinates and Equivalent Isotropic Displacement Parameters ($U_{eq}$) of $Gd_6FeBi_2$ at 210 K and 290 K.

| Atom | site | *x* | *y* | *z* | $U_{eq}$ (Å$^2$) |
|---|---|---|---|---|---|
| 210 K | | | | | |
| Bi1 | 2*d* | 2/3 | 1/3 | 1/2 | 0.0054(4) |
| Gd1 | 3*g* | 0.2382(2) | 0 | 1/2 | 0.0072(4) |
| Gd2 | 3*f* | 0.5984(2) | 0 | 0 | 0.0061(4) |
| Fe1 | 1*a* | 0 | 0 | 0 | 0.0124(19) |
| 290 K | | | | | |
| Bi1 | 2*d* | 2/3 | 1/3 | 1/2 | 0.0111(3) |
| Gd1 | 3*g* | 0.2375(2) | 0 | 1/2 | 0.0135(4) |
| Gd2 | 3*f* | 0.5986(2) | 0 | 0 | 0.0131(4) |
| Fe1 | 1*a* | 0 | 0 | 0 | 0.0189(15) |

**Table S3.** Atomic displacement parameters (Å$^2$) at 120 K, 210 K and 290 K.

| Atom | $U^{11}$ | $U^{22}$ | $U^{33}$ | $U^{12}$ | $U^{13}$ | $U^{23}$ |
|---|---|---|---|---|---|---|
| 120 K | | | | | | |
| Bi1 | 0.0058(6) | 0.0058(6) | 0.0048(8) | 0.0029(3) | 0 | 0 |
| Gd1 | 0.0055(7) | 0.0047(9) | 0.0112(8) | 0.0023(5) | 0 | 0 |
| Gd2 | 0.0069(7) | 0.0064(9) | 0.0049(8) | 0.0032(4) | 0 | 0 |
| Fe1 | 0.016(3) | 0.016(3) | 0.006(4) | 0.0078(15) | 0 | 0 |
| 210 K | | | | | | |
| Bi1 | 0.0073(7) | 0.0073(7) | 0.0079(9) | 0.0036(3) | 0 | 0 |
| Gd1 | 0.0081(9) | 0.0083(11) | 0.0142(10) | 0.0042(5) | 0 | 0 |
| Gd2 | 0.0108(9) | 0.0086(10) | 0.0072(9) | 0.0043(5) | 0 | 0 |
| Fe1 | 0.017(3) | 0.017(3) | 0.005(4) | 0.0084(16) | 0 | 0 |
| 290 K | | | | | | |
| Bi1 | 0.0108(5) | 0.0108(5) | 0.0117(6) | 0.0054(2) | 0 | 0 |
| Gd1 | 0.0099(6) | 0.0099(6) | 0.0214(7) | 0.0055(7) | 0 | 0 |
| Gd2 | 0.0137(6) | 0.0137(6) | 0.0127(6) | 0.0075(6) | 0 | 0 |
| Fe1 | 0.024(2) | 0.024(2) | 0.009(3) | 0.0119(12) | 0 | 0 |

**Table S4**. Selected bond lengths at 210 K and 290 K**.**

| | | | |
|---|---|---|---|
| 210 K | | | |
| Bi1–Gd1 (×3) | 3.2614(8) | Gd1–Gd1 (×2) | 3.441(2) |
| Bi1–Gd2 (×6) | 3.3156(5) | Gd1–Gd2 (×4) | 3.6117(10) |
| Fe1–Gd1 (×6) | 2.9051(8) | Gd1–Gd2 (×2) | 3.6860(15) |
| Fe1–Gd2 (×3) | 3.3582(14) | | |
| 290 K | | | |
| Bi1–Gd1 (×3) | 3.2645(11) | Gd1–Gd1 (×2) | 3.441(2) |
| Bi1–Gd2 (×6) | 3.3181(7) | Gd1–Gd2 (×4) | 3.6111(13) |
| Fe1–Gd1 (×6) | 2.9054(11) | Gd1–Gd2 (×2) | 3.6921(19) |
| Fe1–Gd2 (×3) | 3.3568(17) | | |

**Table S5.** Hirshfeld analysis from DFT calculations.

| Atom | Hirsheld charge (e) | Spin ($\hbar/2$) |
|---|---|---|
| Fe | –0.24 | –2.03 |
| Gd1 | –0.01 | 7.96 |
| Gd2 | 0.05 | 7.84 |
| Bi | –0.08 | 0.11 |

**Table S6.** Bond population analysis from DFT calculations.

| Bond | Population |
|---|---|
| Fe–Gd1 | 0.62 |
| Fe–Gd2 | 0.35 |
| Bi–Gd1 | –1.15 |
| Bi–Gd2 | –1.08 |